Supporting Information

Charge Transport and Glassy Dynamics in Polymeric Ionic Liquids as reflected by its inter- and intramolecular Interactions

F. Frenzel[1], P. Borchert[2], A. M. Anton[1], V. Strehmel[2] and F. Kremer[1]

[1]Leipzig University, Peter-Debye Institute for Soft Matter Physics, Linnèstraße 5, 04103 Leipzig, Germany

[2]Niederrhein University of Applied Sciences, Institute for Coatings and Surface Chemistry, Adlerstraße 32, 47798 Krefeld, Germany

(1) Experimental section:

- *Intrinsic viscosities:* [η] of the homopolymers were measured using an Ubbelohde viscosimeter with a capillary constant of 0,0097854 mm²/s². A LAUDA iVisc was used for the measurements and a LAUDA viscocool 6 was used for sample tempering. Solutions for the measurements were prepared from identical stock solutions. Poly (1-butyl-3-methylimidazolium styrene sulfonate) was dissolved in 0.05 M 1-butyl-3-methylimidazolium chloride solution in H_2O for 24 h at room temperature. Poly (1-butyl-3-vinylimidazolium bis(trifluoromethylsulfonyl)imide) was dissolved in 0.075 M lithium bis(trifluoromethylsulfonyl)imide solution in methylethylketone for 24 h at room temperature. Poly (*N*-butyl-*N,N*-dimethyl-ammonium bis(trifluoromethylsulfonyl)imide) was dissolved in 0.15 M lithium bis(trifluoromethylsulfonyl)imide solution in methylethylketone for 24 h at room temperature as well. Measured data were corrected using the *Hagenbach* correction method. Intrinsic viscosities [η] were determined from the plot of reduced viscosity data (η_{spec}/c) as function of the concentration using linear regression with the y-axis at zero concentration.

  Reference: J. Brandrup, E.H. Immergut Polymer Handbook, *Wiley-Interscience, New York*, **1975**.

- The synthesis of 1-butyl-3-vinylimidazolium bis(trifluoromethylsulfonyl)imide involved a two-step reaction beginning with quaternization of equimolar amounts of 1-vinylimidazole and 1-iodobutane followed by anion exchange with lithium bis(trifluoromethylsulfonyl)imide. 1-Vinylimidazole (72.7 g, 0.77 mol) was dissolved in 50 ml tert-butyl methyl ether. 1-Iodobutane (142.3 g, 0.77 mol) was added dropwise to this solution, and it was stirred at room temperature for 7 d. The mixture separated into two phases. The organic phase was washed with ethyl acetate (3 × 50 ml) and dried under vacuum for 2 d. Yield: 183.4 g, 85 %. T_m = 19 °C.

  ¹H NMR (300 MHz, Acetone-d_6): δ (ppm) = 10.33 (s, 1H, N–CH–N), 8.38 (t, *J* = 1.8 Hz, 1H, N–CH), 8.15 (t, *J* = 1.7 Hz, 1H, N–CH), 7.61 (dd, *J* = 15.7, 8.8 Hz, 1H, CH_{vinyl}), 6.23 (dd, *J* = 15.7, 2.6 Hz, 1H, CH_{vinyl}), 5.47 (dd, *J* = 8.8, 2.6 Hz, 1H, CH_{vinyl}), 4.55 (t, *J* = 7.3 Hz, 2H, N–CH_2), 2.12 – 1.95 (m, 2H, CH_2), 1.52 – 1.35 (m, 2H, CH_2), 0.96 (t, *J* = 7.4 Hz, 3H, CH_3). **¹³C NMR** (75 MHz, Acetone-d_6): δ (ppm) = 136.10 (N–CH–N), 129.51 (N–CH), 124.04 (N–CH), 120.39 (CH_{vinyl}), 109.52 (CH_{2vinyl}), 50.24 (N–CH_2), 32.42 (CH_2), 19.75 (CH_2), 13.63 (CH_3). Lithium bis(trifluoromethylsulfonyl)imide (202.5 g, 0.705 mol) was dissolved in 60 ml water and added dropwise to a solution of 1-butyl-3-vinylimidazolium iodide(183.4 g, 0.66 mol) in 60 ml water. The reaction mixture was stirred at room temperature for 12 h. The water phase was decanted, and the product was washed with fresh water (5 × 50 ml) until no AgI was detected. Yield: 268.4 g, 94% (H_2O content: 0.05%; T_g = -15 °C).

  ¹H NMR (300 MHz, CD_3CN):δ(ppm) = 8.72 (s, 1H, N–CH–N), 7.69 (t, *J* = 1.8 Hz, 1H, N–CH), 7.49 (t, *J* = 1.7 Hz, 1H, N–CH), 7.10 (dd, *J* = 15.6, 8.7 Hz, 1H, CH_{vinyl}), 5.79 (dd, *J* = 15.6, 2.8 Hz, 1H, CH_{vinyl}), 5.41 (dd, *J* = 8.7, 2.7 Hz, 1H, CH_{vinyl}), 4.17 (t, *J* = 7.3 Hz, 2H, N–CH_2), 1.92 – 1.77 (m, 2H, CH_2), 1.36 (dd, *J* = 15.2, 7.5 Hz, 2H, CH_2), 0.95 (t, *J* = 7.3 Hz, 3H, CH_3). **¹³C NMR** (75 MHz, CD_3CN): δ (ppm) = 134.36 (N–CH–N), 128.46 (N–CH), 123.14 (N–CH), 122.07

(CF$_3$), 119.49 (CH$_{vinyl}$), 109.22 (CH$_{2vinyl}$), 49.75 (N–CH$_2$), 31.35 (CH$_2$), 18.98 (CH$_2$), 12.65 (CH$_3$).

- Silver *p*-styrenesulfonate was prepared by reacting equimolar quantities of sodium *p*-styrenesulfonate (40.0 g, 0.194 mol) with silver nitrate (33.0 g, 0.194 mol) that were separately dissolved in distilled water (200 mL and 33 mL). The reaction was carried out during stirring and in the absence of light for 2 h at room temperature. The precipitated monomer was filtrated, washed with water (3 x 50 mL), and dried under vacuum at 40 °C for 48 h resulting in silver-*p*-styrene sulfonate as a white solid (yield: 50 g, 88 %).

  1-Butyl-3-methylimidazolium chloride was synthesized in bulk: 1-chlorobutane (102.0 g, 1.1 mol) was added to 1-methylimidazole (82.0 g, 1 mol) under stirring. The reaction was carried out for 14 d at 70 °C until the quaterinzation of 1-methylimidole was complete. This was verified by ^{1}H NMR. 1-Butyl-3-methylimidazolium chloride was washed with ethyl acetate (4 x 50 mL), and dried for 48 h in vacuo to give a white solid (Yield: 150.2 g, 86%).

  ^{1}H NMR (300 MHz, D$_2$O): δ (ppm) = 8.76 (s, 1H, N–CH–N), 7.51 (t, *J* = 1.7 Hz, 1H, N–CH), 7.46 (t, *J* = 1.7 Hz, 1H, N–CH), 4.22 (t, *J* = 7.1 Hz, 2H, N–CH$_2$), 3.92 (s, 3H, N–CH$_3$), 1.87 (dt, *J* = 20.2, 7.3 Hz, 2H, CH$_2$), 1.41 – 1.25 (m, 2H, CH$_2$), 0.93 (t, *J* = 7.4 Hz, 3H, CH$_3$). **^{13}C NMR** (75 MHz, D$_2$O): δ (ppm) = 135.86 (N–CH–N), 123.51 (N–CH), 122.26 (N–CH), 49.31 (N–CH$_2$), 35.71 (N–CH$_3$), 31.31 (CH$_2$), 18.79 (CH$_2$), 12.71 (CH$_3$).

  Silver-*p*-styrenesulfonate (11.01 g, 37.8 mmol) was suspended in methanol (50 mL) followed by addition of a methanolic solution of 1-butyl-3-methylimidazolium chloride (6.29 g, 36 mmol; dissolved in 20 mL methanol). The solution was purged with nitrogen to remove residual oxygen, and it was kept under argon for the entire reaction time. The solution was stirred for 2 h at room temperature resulting in precipitation of silver chloride. The precipitate was filtered off and washed with methanol (4 x 25 mL). The methanolic solutions were unified, and the solvent was removed under reduced pressure. The product was dried for 24 h in vacuo (yield: 10.37 g, 89 %). The 1-butyl-3-methylimidazolium styrenesulfonate was obtained as a white solid (H$_2$O content: 0.09%; T$_g$ = -15 °C, T$_m$ = 45 °C).

  ^{1}H NMR (300 MHz, MeOD): δ (ppm) = 8.91 (s, 1H, N–CH–N), 7.78 (d, *J* = 8.3 Hz, 2H, aromatic-CH$_2$), 7.58 (t, *J* = 1.6 Hz, 1H, N–CH–N), 7.50 (d, *J* = 8.3 Hz, 2H, aromatic-CH$_2$), 6.77 (dd, *J* = 17.6, 11.0 Hz, 1H, N–CH), 5.87 (dd, *J* = 17.6, 0.5 Hz, 1H, CH$_{vinyl}$), 5.32 (d, *J* = 11.0 Hz, 1H, CH$_{vinyl}$), 4.85 (s, 1H, CH$_{vinyl}$), 4.15 (t, *J* = 7.3 Hz, 2H, N–CH$_2$), 3.88 (s, 3H, N–CH$_3$), 1.86 – 1.73 (m, 2H, CH$_2$), 1.38 – 1.23 (m, 2H, CH$_2$), 0.94 (t, *J* = 7.4 Hz, 3H, CH$_3$). **^{13}C NMR** (75 MHz, MeOD): δ (ppm) = 145.73 (N–CH–N), 140.73(C$_q$), 137.72 (aromatic-CH$_2$), 137.10 (N–CH–N), 127.10 (d *J* = 10.4 Hz, C$_q$, CH$_{vinyl}$), 124.84 (aromatic–CH$_2$), 123.53 (N–CH), 115.99 (CH$_{vinyl}$), 50.45 (N–CH$_2$), 36.45(N–CH$_3$), 32.99 (CH$_2$), 20.35 (CH$_2$), 13.76 (CH$_3$).

- chemical NMR shift *N*-butyl-*N,N*-dimethyl-ammonium bis(trifluoromethylsulfonyl)imide: **^{1}H NMR** (300 MHz, CD$_3$CN): δ (ppm) = 6.10 – 6.08 (m, 1H, CH$_{vinyl}$), 5.71 – 5.68 (m, 1H, CH$_{vinyl}$), 4.51 – 4.44 (m, 2H, CH$_2$), 3.62 – 3.56 (m, 2H, CH$_2$), 3.32 – 3.23 (m, 2H, CH$_2$), 3.04 (s, 6H, 2 x N–CH$_3$), 1.93 – 1.92 (m, 3H, CH$_3$), 1.69 (d, *J* = 8.3 Hz, 2H, O-CH$_2$), 1.34 (dd, *J* = 14.9, 7.4 Hz, 2H, N–CH$_2$), 0.95 (t, *J* = 7.3 Hz, 3H, C$_q$–CH$_3$). **^{13}C NMR** (75 MHz, CD$_3$CN): δ (ppm) = 166.17 (C=O), 135.80 (C$_q$–vinyl), 126.27 (d, J = 8.2 Hz, C$_q$–vinyl), 122.08 (CH$_{vinyl}$), 117.38 (CF$_3$), 65.20 (O–CH$_2$), 62.91 – 62.37 (N–CH$_2$), 57.83 (N–CH$_2$), 51.48 – 51.04 (2 x N–CH$_3$), 24.10 (CH$_2$), 19.21 (CH$_3$–C$_q$), 17.34 (CH$_2$), 12.77 (CH$_3$).
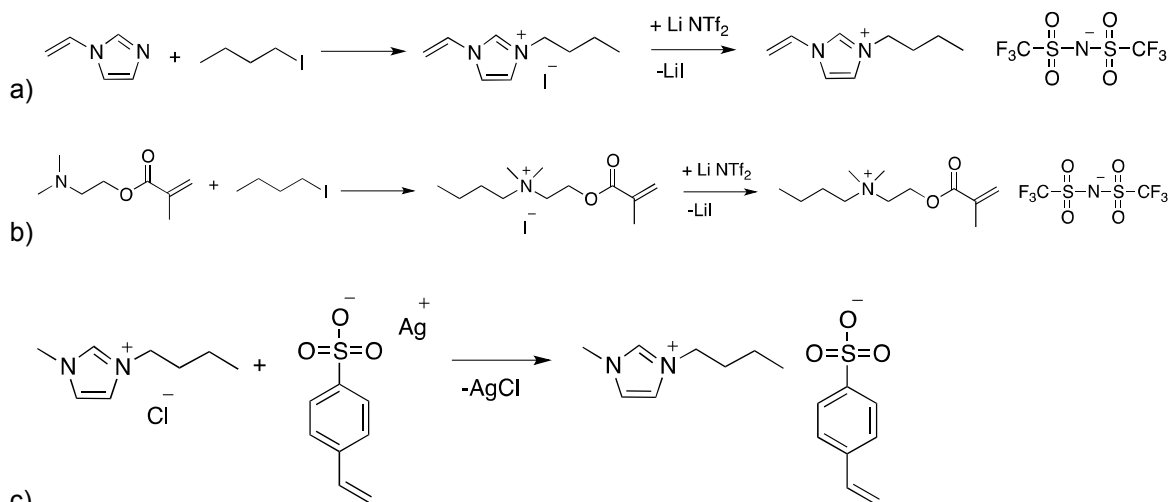
Scheme 1: Synthesis of ionic liquid monomers based on a) 1-vinylimidazole, b) 2-(dimethylamino)ethyl methacrylate, and c) styrene sulfonate. The first step of the synthesis involved quaternization with 1-iodobutane in the case of a) + b), and 1-chlorobutane in the case of c), followed by anion metathesis with Lithium bis(trifluoromethylsulfonyl)imide (a + b) and Silver-*p*-styrenesulfonate (c).
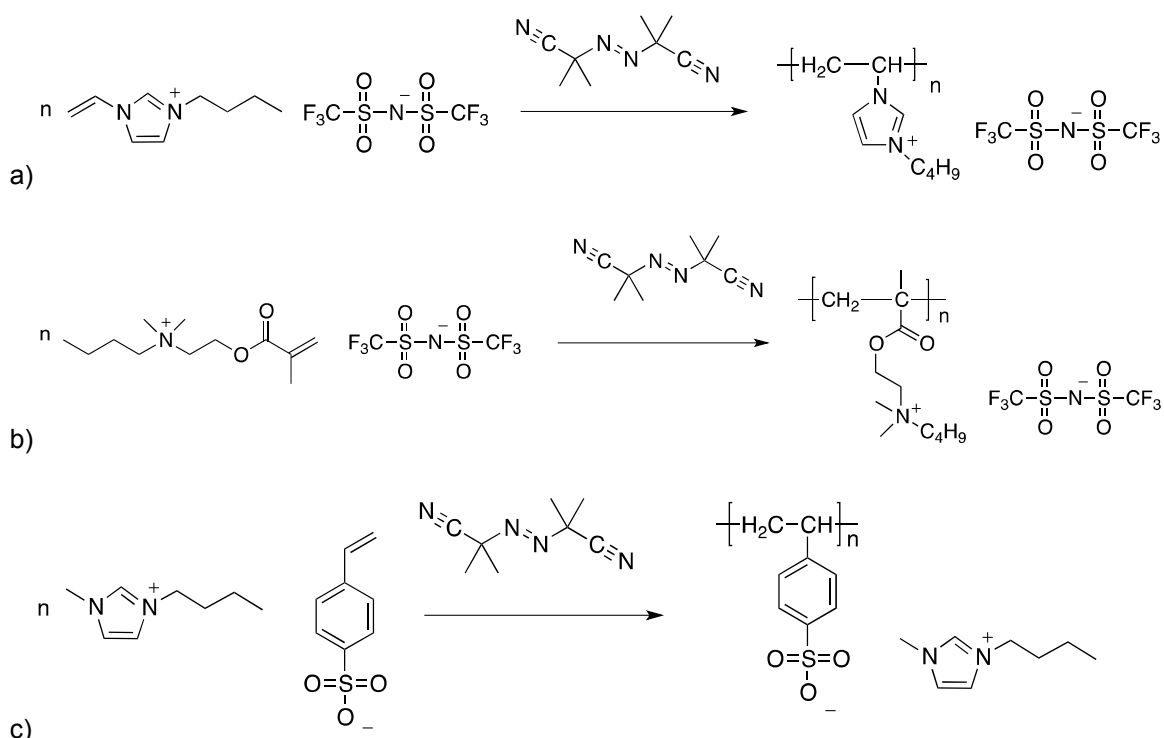
Scheme 2: Synthesis of homopolymers of ionic liquid monomers via free radical polymerization.

(2) Additional Characterization:

- NMR-spectra of the ionic liquid monomers:
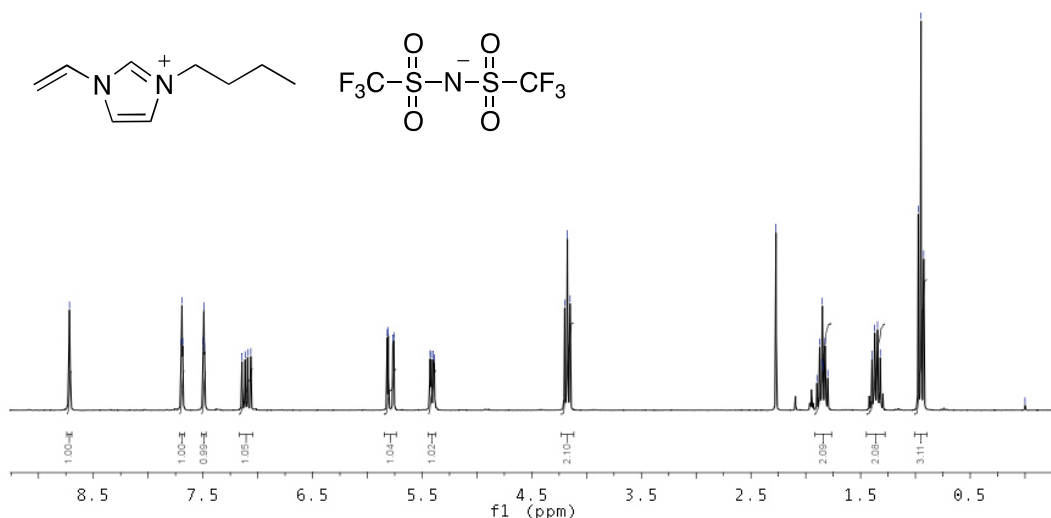
Figure S1: ^{1}H NMR spectrum of 1-Butyl-3-vinylimidazolium bis(trifluoromethylsulfonyl)imide in CD$_3$CN.
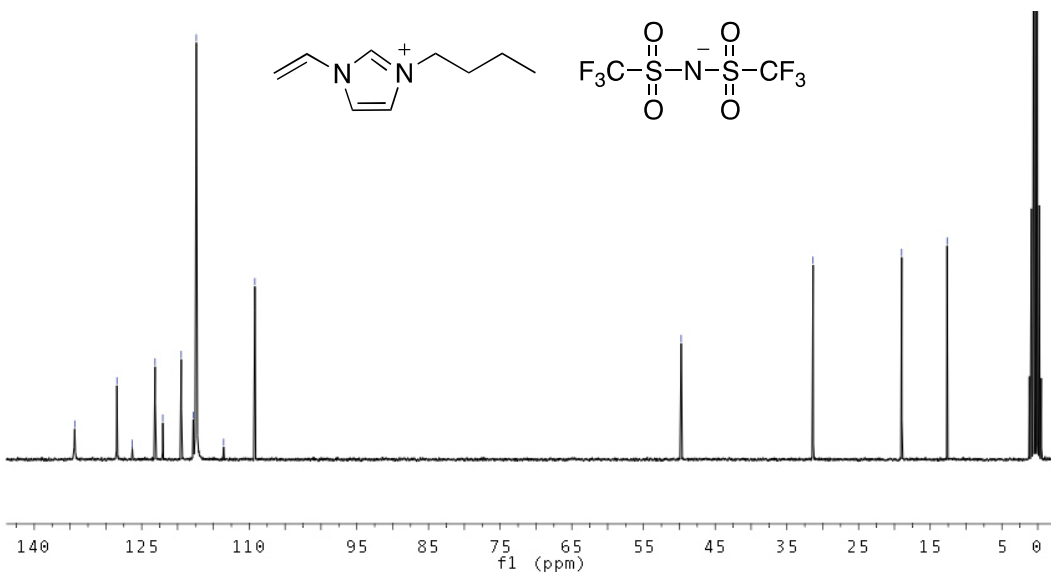
Figure S2: ^{13}C NMR spectrum of 1-Butyl-3-vinylimidazolium bis(trifluoromethylsulfonyl)imide in CD$_3$CN.
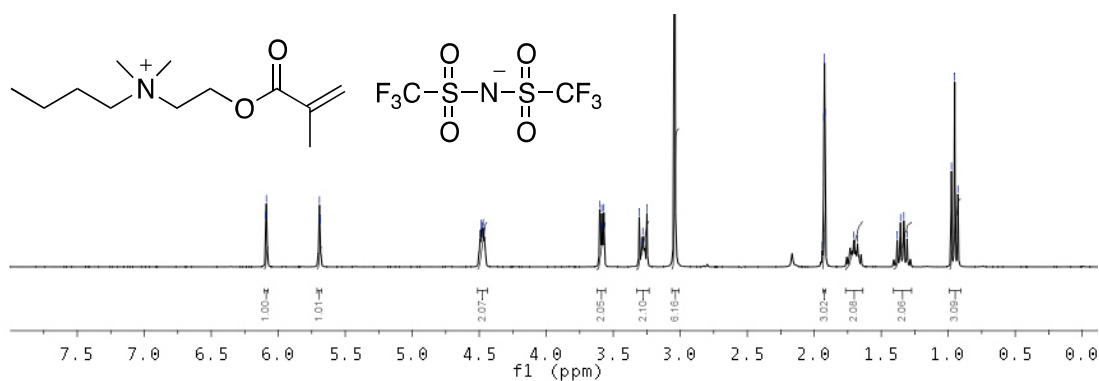
Figure S3: ^{1}H NMR spectrum of N-butyl-N,N-dimethyl-ammonium bis(trifluoromethylsulfonyl)imide in CD$_3$CN.
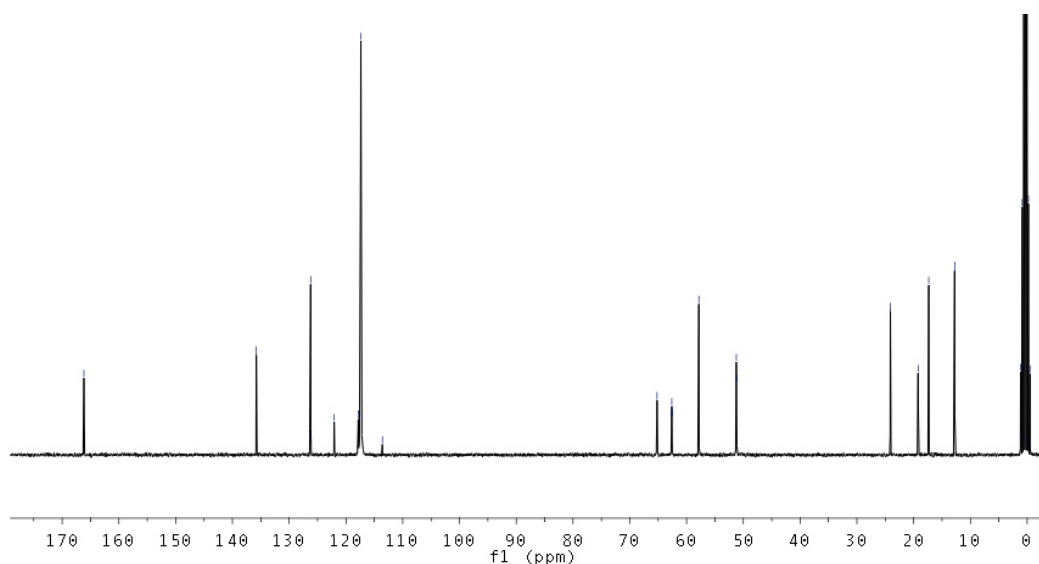
Figure S4: ^{13}C NMR spectrum of N-butyl-N,N-dimethyl-ammonium bis(trifluoromethylsulfonyl)imide in CD_3CN.
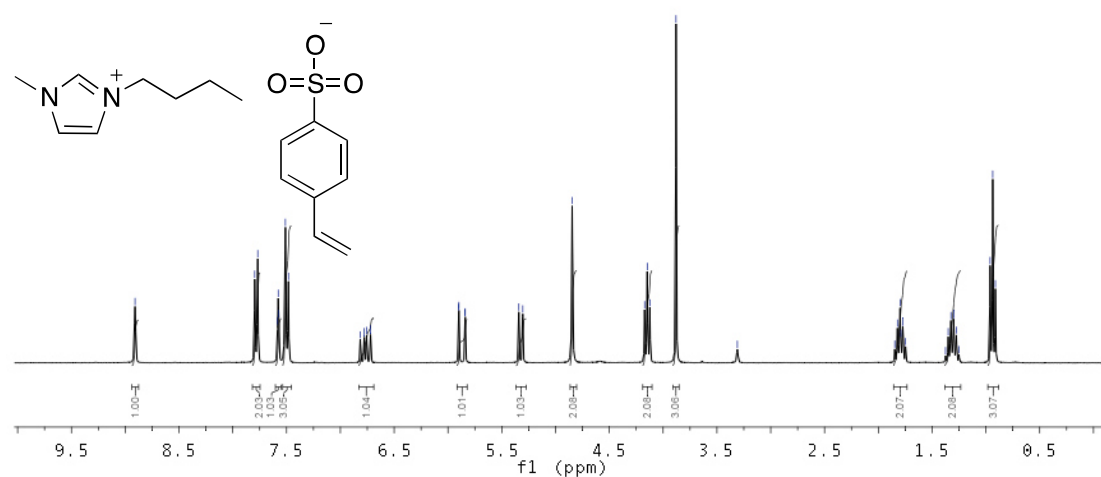
Figure S5: ^1H NMR spectrum of 1-Butyl-3-methylimidazolium styrenesulfonate in MeOD.
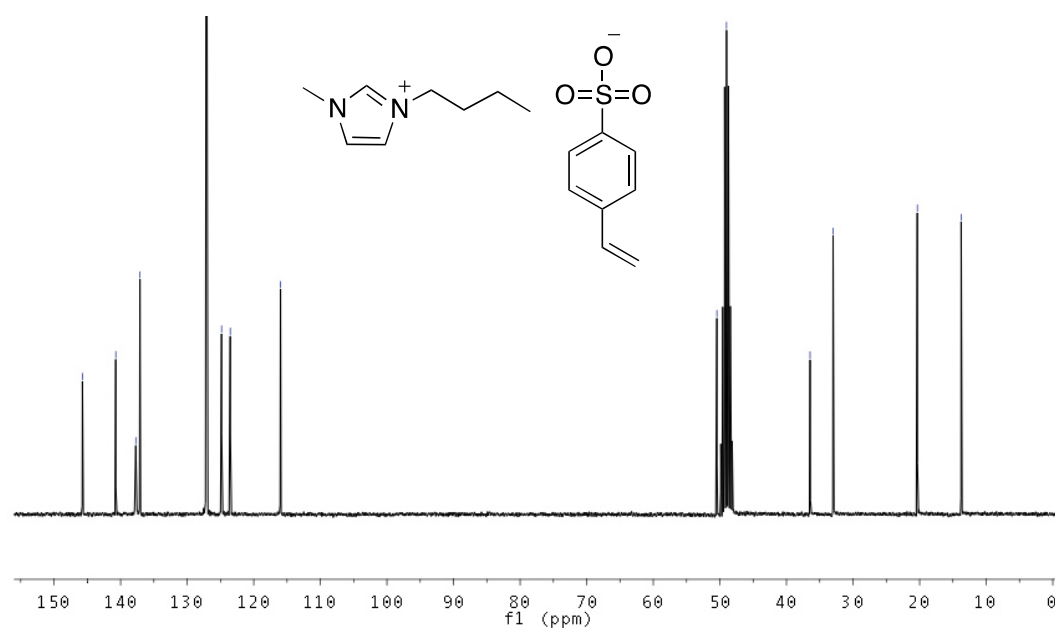
Figure S6: ^{13}C NMR spectrum of 1-Butyl-3-methylimidazolium styrenesulfonate in MeOD.

- NMR-spectra of the polymerized ionic liquids:
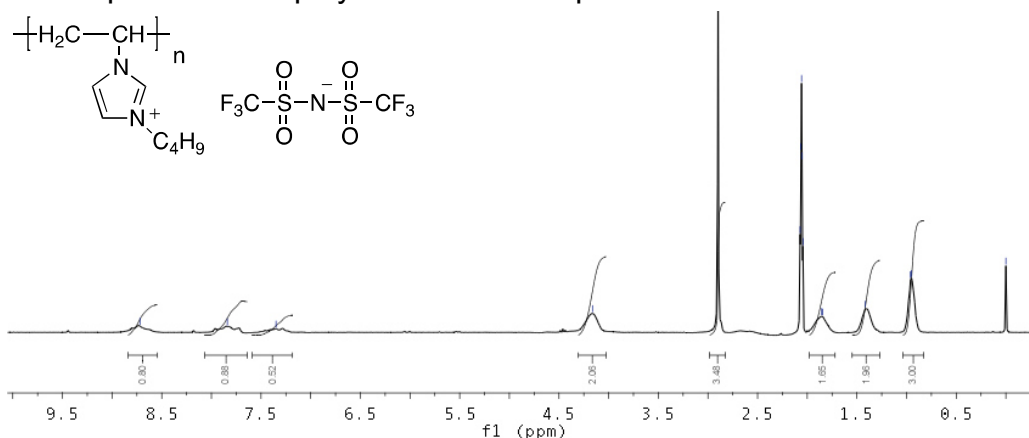
Figure S7: ^{1}H NMR spectrum in CD$_3$CN of polymeric 1-butyl-3-vinylimidazolium bis(trifluoromethylsulfonyl)imide after purification. The proton signals of the vinyl group between 5.4 ppm and 5.7 ppm are not existing, since conversion of double bonds was complete.
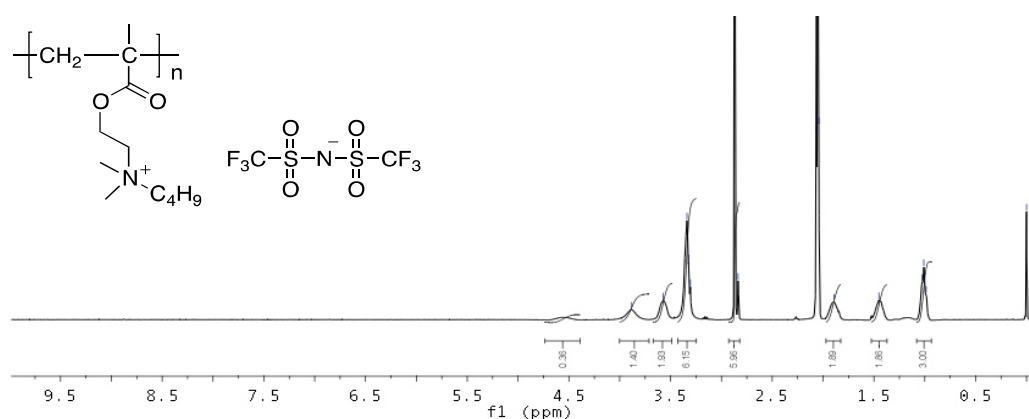
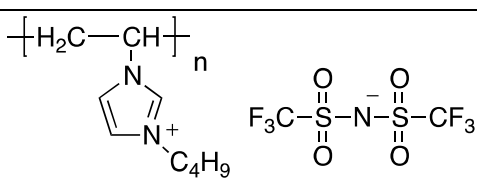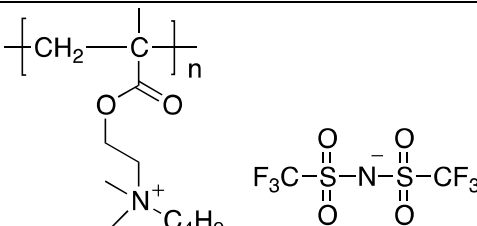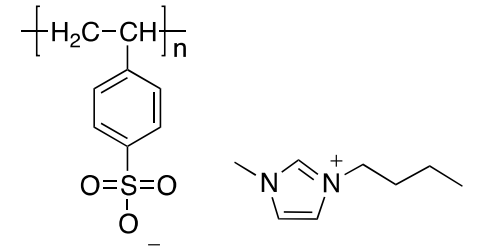**Figure S8:** ^{1}H NMR spectrum in CD$_3$CN of polymeric *N*-butyl-*N,N*-dimethyl-ammonium bis(trifluoromethylsulfonyl)imide after bulk polymerization and washing with methanol and vacuum-drying. The proton signals of the vinyl group between 5.7 ppm and 6.1 ppm are not existing, since conversion of double bonds was complete.
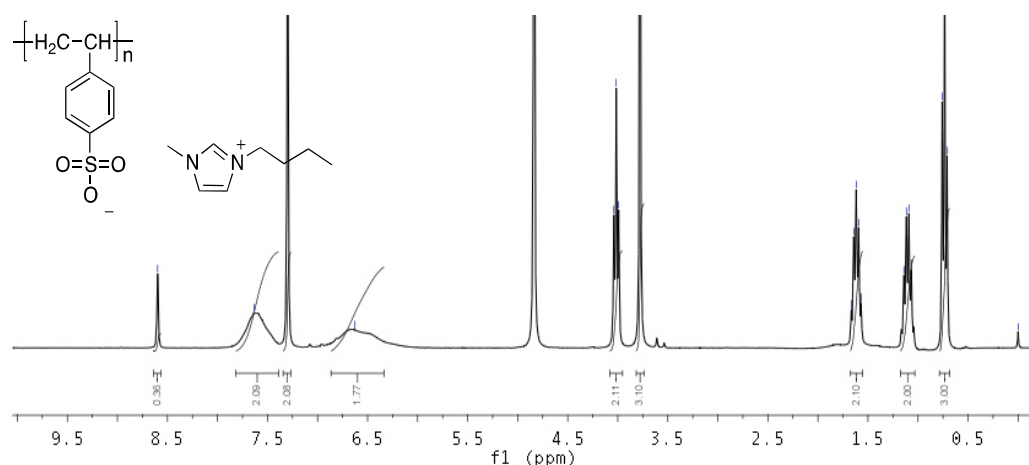
Figure S9: ^{1}H NMR spectrum in MeOD of polymeric 1-butyl-3-methylimidazolium styrenesulfonate after bulk polymerization and purification. The sharp proton signals are caused by the 1-butyl-3-methylimidazolium, since this cation is not part of the polymer chain. The broad signals at 6.5 ppm and 7.7 ppm are protons of the benzene ring.

- intrinsic viscosities of the PILs under study:

The different polymers investigated were obtained similarly by free radical polymerization using 4,4'-azobisisobutyronitrile as thermal initiator. The homopolymers were synthesized in an inert atmosphere, and the polymerization time was 24 h. Due to structural variances, the intrinsic viscosities differ significantly. The *Schulz-Blaschke* and the *Huggins* values are comparable for each polymer solution investigated. The intrinsic viscosity increases from poly (1-butyl-3-vinylimidazolium bis(trifluoromethylsulfonyl)imide) to poly (*N*-butyl-*N,N*-dimethyl-ammonium bis(trifluoromethyl- sulfonyl)imide). The polymerizable functional group changes from a vinyl-group to a methacrylate-group, and the anion changes as well. Therefore, different parameters – such as counterions, functional groups, and solvents – influence the intrinsic viscosities.

Table 1: Molecular weight determined by intrinsic viscosity of the investigated homopolymers.

Polymer	Intrinsic viscosity [ml/g]
	$[\eta]_{Huggins} = 34.07$ $[\eta]_{Schulz-Blaschke} = 33.74$
	$[\eta]_{Huggins} = 98.11$ $[\eta]_{Schulz-Blaschke} = 99.62$
	$[\eta]_{Huggins} = 395.62$ $[\eta]_{Schulz-Blaschke} = 411.75$

- dielectric overviewspectra:

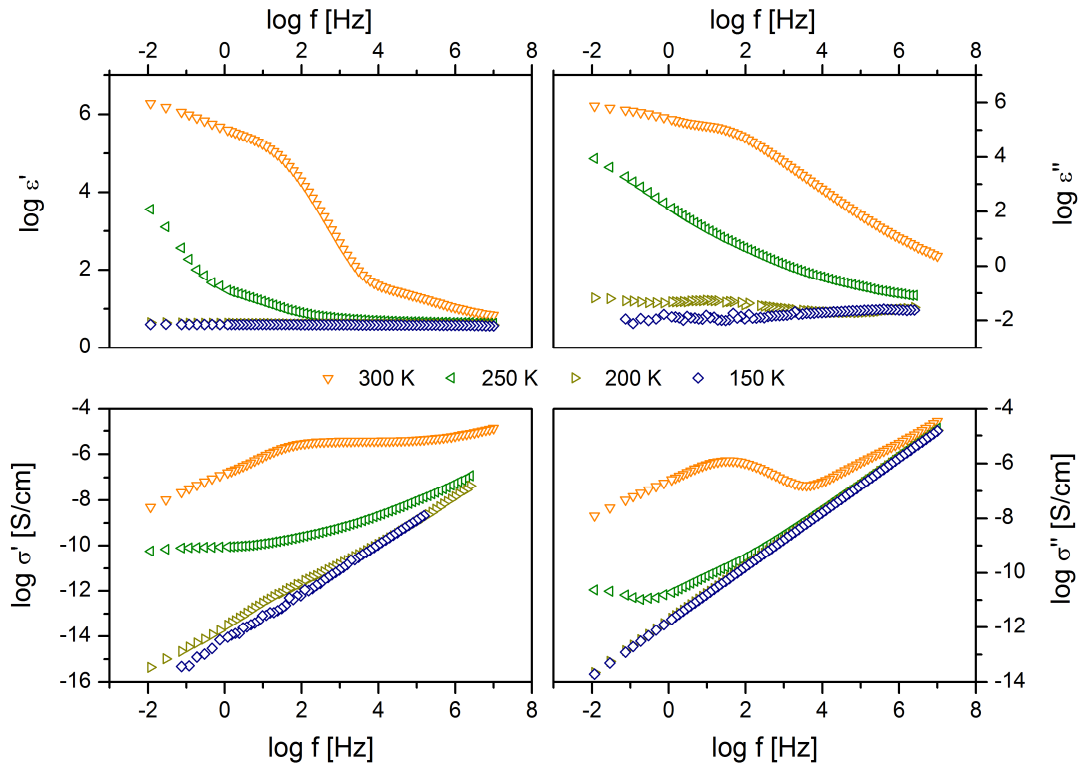**Figure S10**: Real and imaginary part of the complex dielectric function ε*= ε'-iε'' as well as the complex conductivity σ*=σ'+iσ'' *versus* frequency of the sample BMIM-StySu at 4 different temperatures as indicated. The logarithm is to base 10; the error-bars are smaller than the symbols-size, unless explicitly specified otherwise.
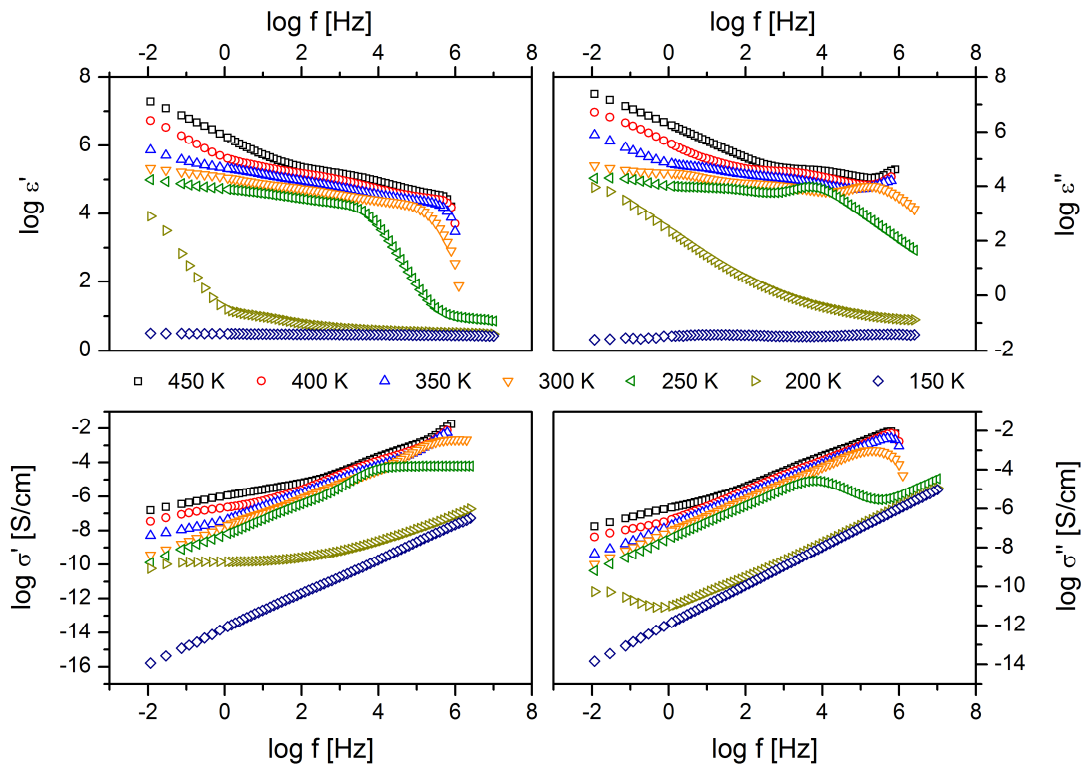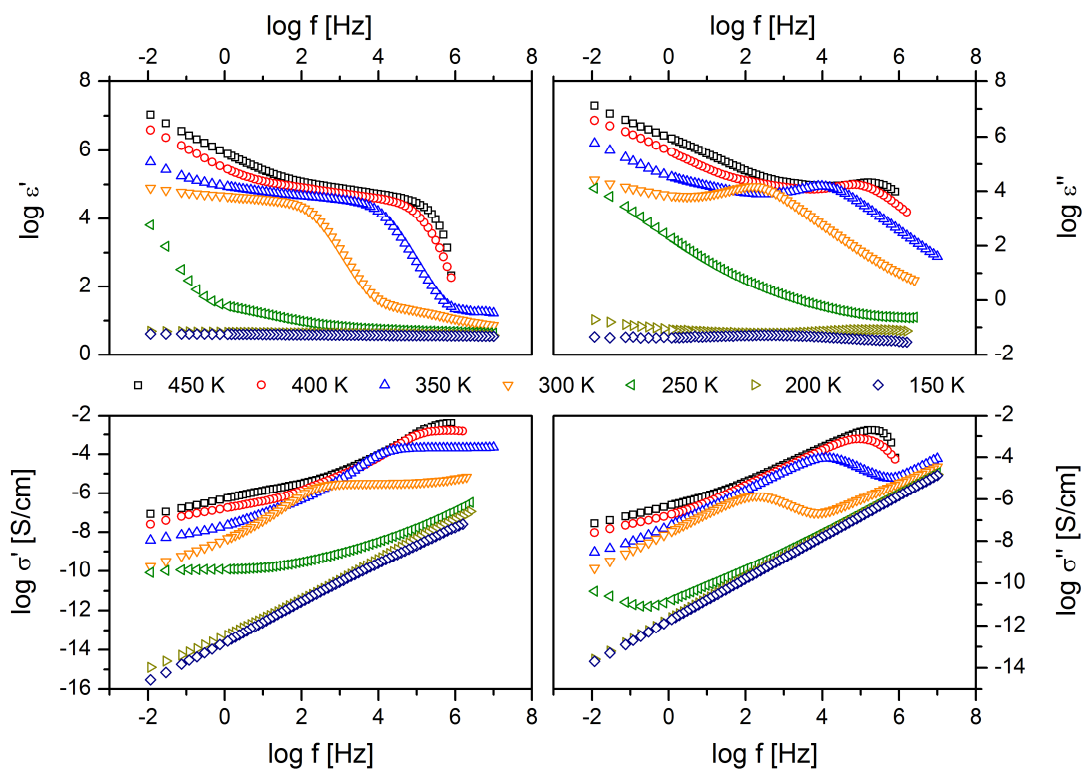

Figure S11: Real and imaginary part of the complex dielectric function ε*= ε'-iε'' as well as the complex conductivity σ*=σ'+iσ'' *versus* frequency of the sample BVIM-NTf₂ at 7 different temperatures as indicated. The logarithm is to base 10; the error-bars are smaller than the symbols-size, unless explicitly specified otherwise.
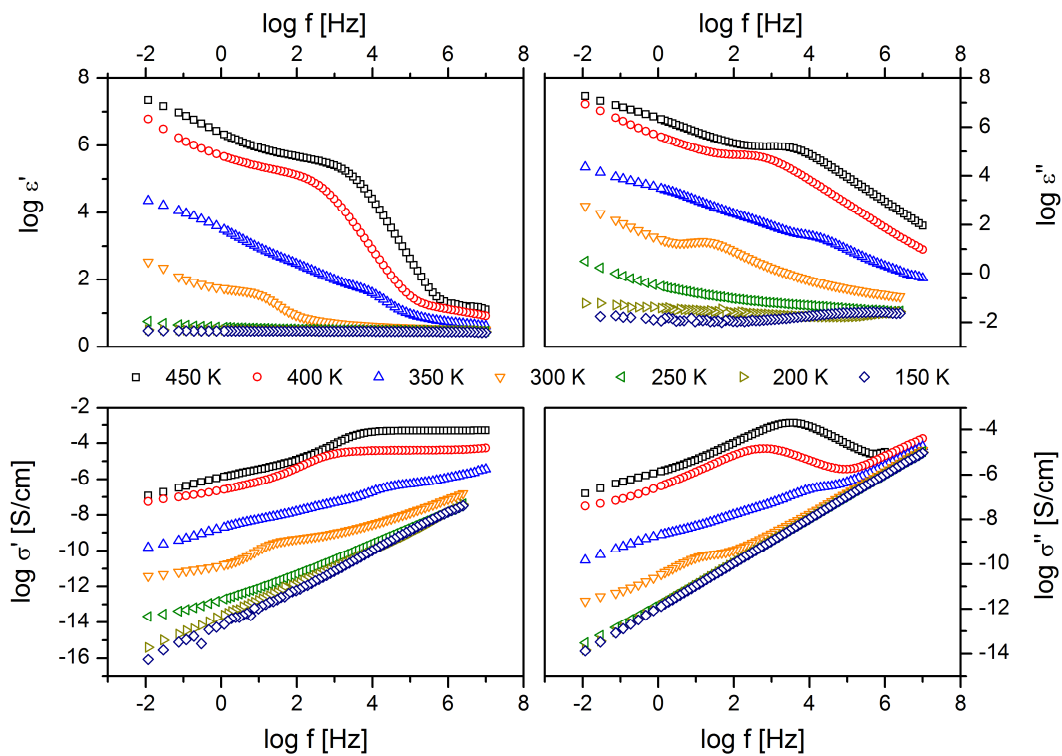
Figure S12: Real and imaginary part of the complex dielectric function $\varepsilon^* = \varepsilon' - i\varepsilon''$ as well as the complex conductivity $\sigma^* = \sigma' + i\sigma''$ *versus* frequency of the sample BDMAEMA-NTf$_2$ at 7 different temperatures as indicated. The logarithm is to base 10; the error-bars are smaller than the symbols-size, unless explicitly specified otherwise.
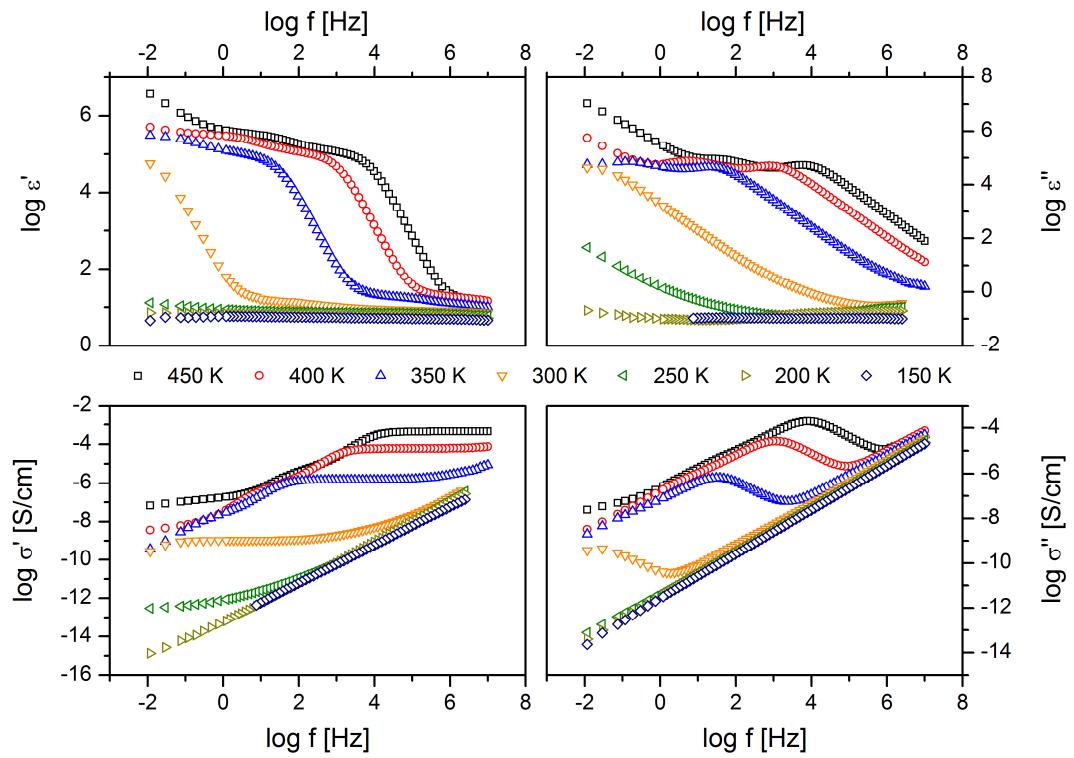

Figure S13: Real and imaginary part of the complex dielectric function $\varepsilon^* = \varepsilon' - i\varepsilon''$ as well as the complex conductivity $\sigma^* = \sigma' + i\sigma''$ *versus* frequency of the sample P[BMIM-StySu] at 7 different temperatures as indicated. The logarithm is to base 10; the error-bars are smaller than the symbols-size, unless explicitly specified otherwise.

Figure S14: Real and imaginary part of the complex dielectric function $\varepsilon^* = \varepsilon' - i\varepsilon''$ as well as the complex conductivity $\sigma^* = \sigma' + i\sigma''$ *versus* frequency of the sample P[BVIM-NTf$_2$] at 7 different temperatures as indicated. The logarithm is to base 10; the error-bars are smaller than the symbols-size, unless explicitly specified otherwise.
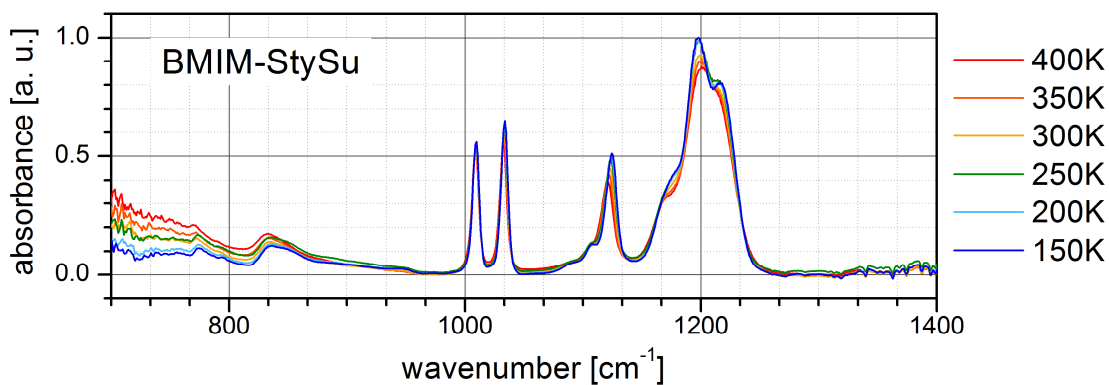
- temperature-dependent IR-spectra:

Figure S15: FTIR absorption-spectra of sample BMIM-StySu at 6 different temperatures as indicated.
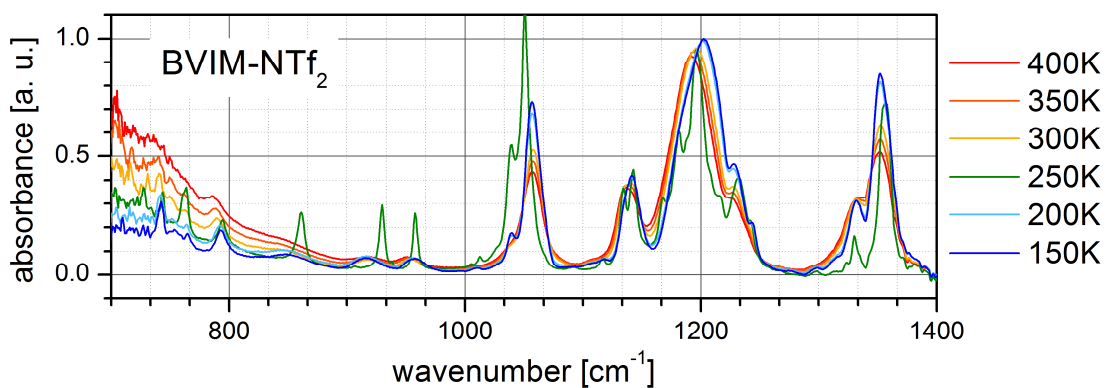
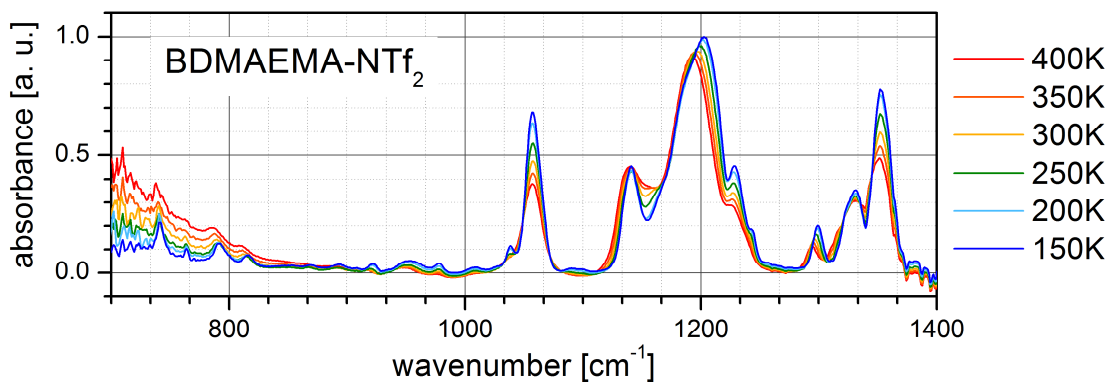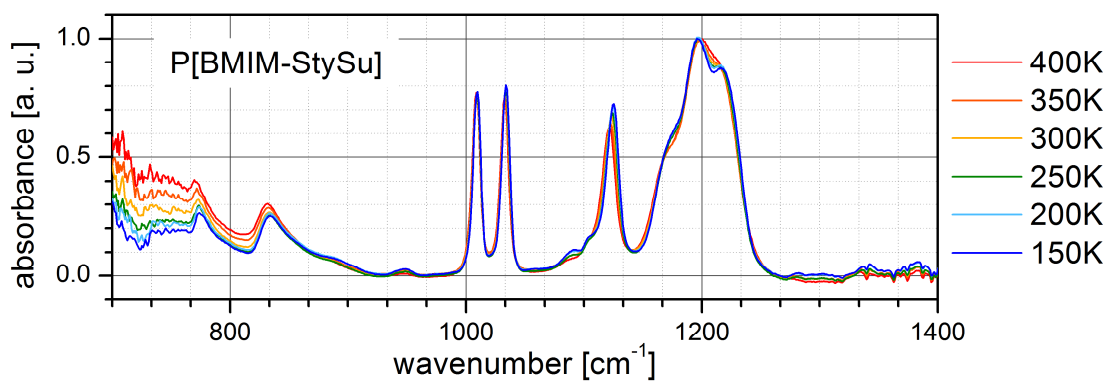**Figure S16**: FTIR absorption-spectra of sample BVIM-NTf$_2$ at 6 different temperatures as indicated.

Figure S17: FTIR absorption-spectra of sample BDMAEMA-NTf$_2$ at 6 different temperatures as indicated.

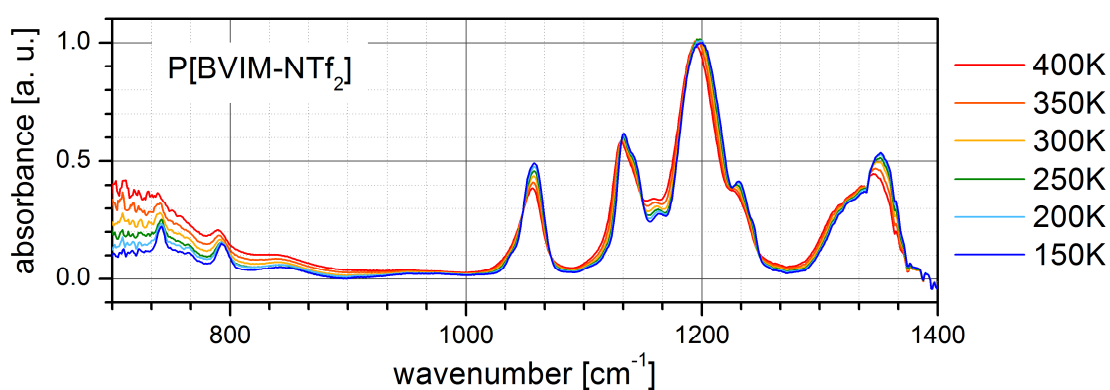**Figure S18**: FTIR absorption-spectra of sample P[BMIM-StySu] at 6 different temperatures as indicated.

Figure S19: FTIR absorption-spectra of sample P[BVIM-NTf$_2$] at 6 different temperatures as indicated.
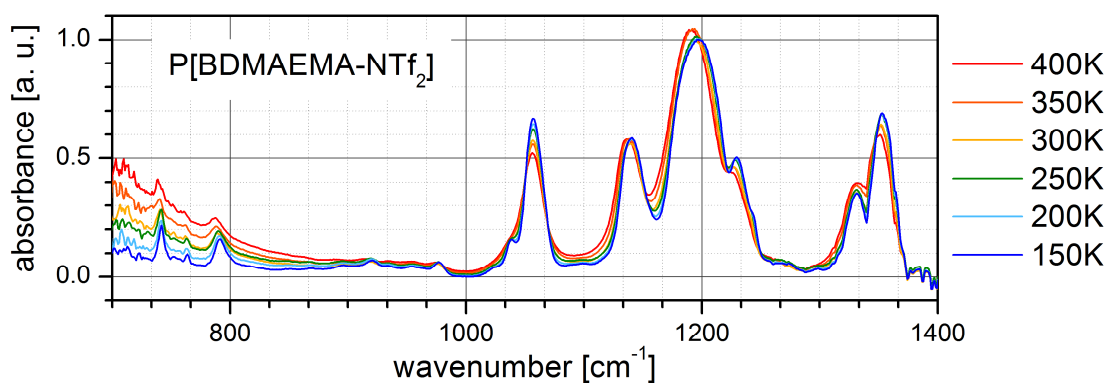

Figure S20: FTIR absorption-spectra of sample P[BDMAEMA-NTf$_2$] at 6 different temperatures as indicated.
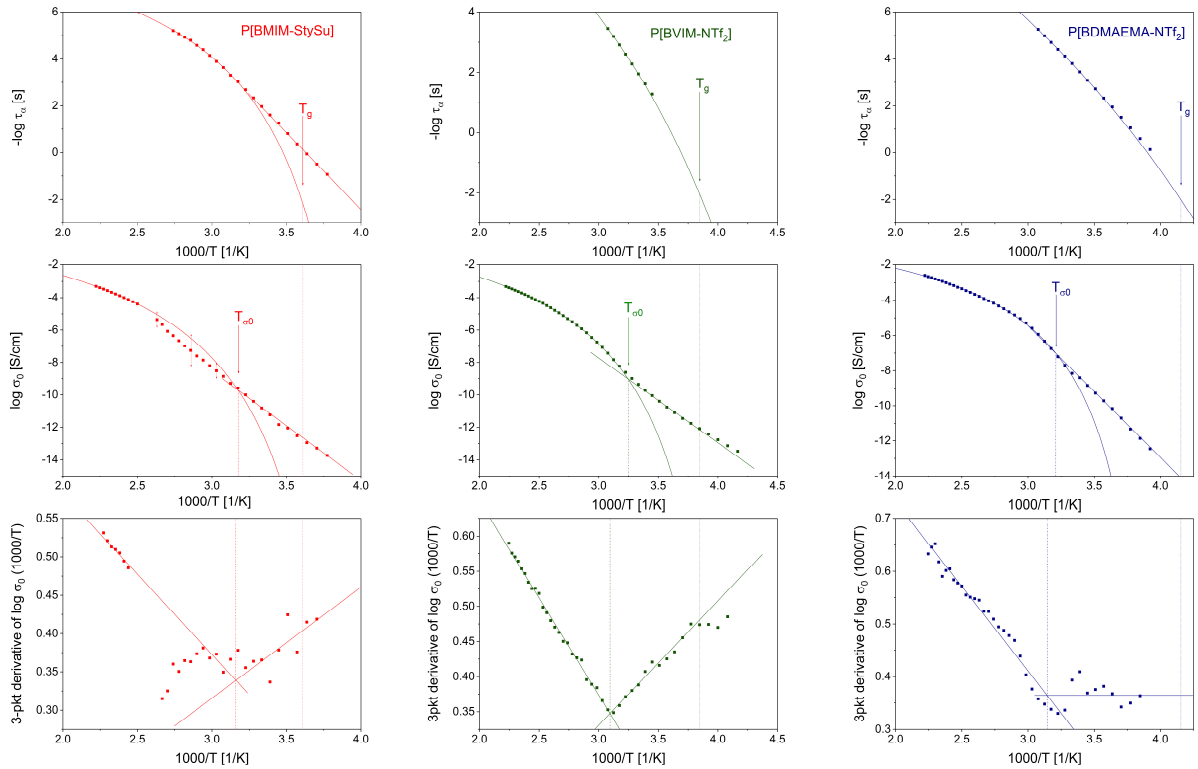
Figure S21: Structural relaxation time τ_α (top row), DC-conductivity σ_0 (middle row) as well as the 3-point first order derivative of σ_0 versus the inverse temperature. The characteristic temperatures T_g (glass transition temperature) $T_{\sigma 0}$ (transition temperature) are indicated in dotted and dashed-dotted lines, respectively.
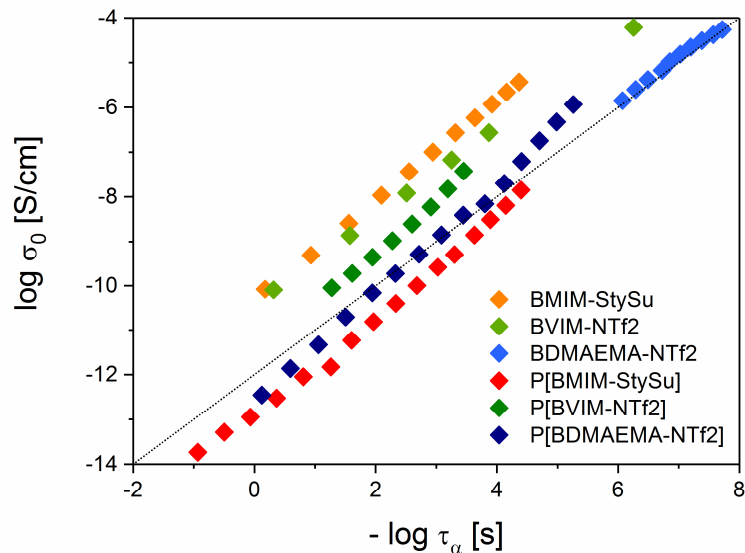

Figure S22: DC-conductivity σ_0 versus the structural relaxation time τ_α, which is molecularly assigned to fluctuations of transient ion pairs determining both the glassy nature of the overall systems as well as charge transport. The dotted line indicates a slope equal 1. The error bars are in the size of the symbols.
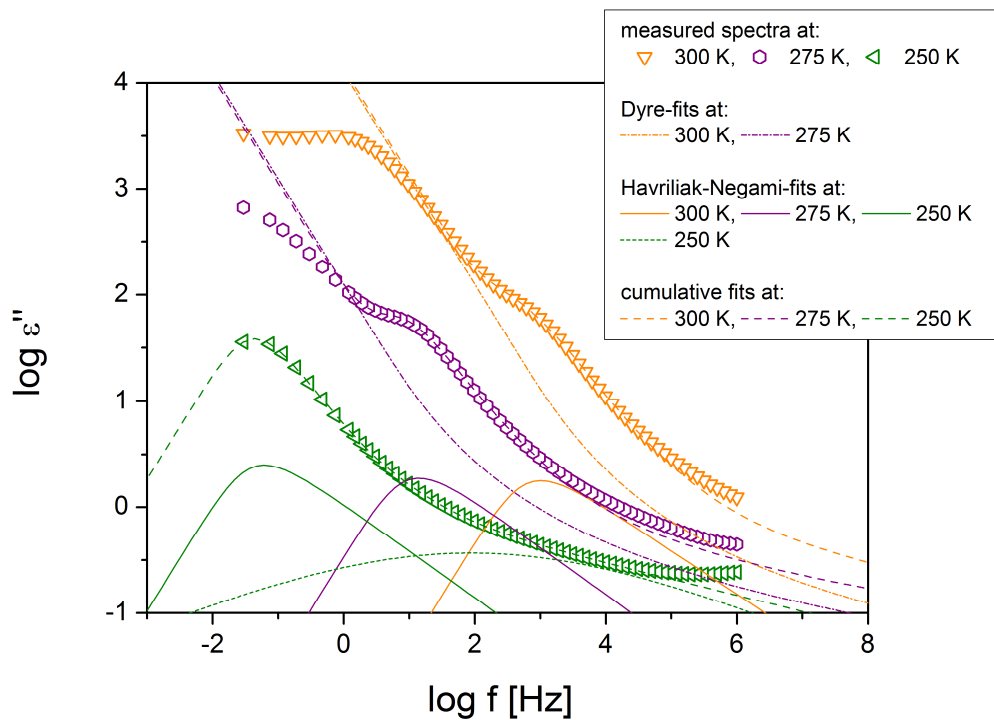
Figure S23: Representative demonstration of the analysis procedure of dielectric data in $\varepsilon''(f)$. To obtain the physical characteristics of the mean relaxation times, the DC-conductivity value as well as the charge carrier hopping rate the dielectric spectra is fitted by a superposition of a Dyre- (dashed-dotted lines) and one or more Havriliak-Negami functions (solid lines: α-process, dotted line: β_1-process) as depicted. The cumulative fits are displayed as dashed lines; deviations to the measurement data originate from unconsidered contributions at the given temperatures. The error bars are in the size of the symbols.